Cell Stress and Chaperones (2020) 25:481–494
https://doi.org/10.1007/s12192-020-01088-y

ORIGINAL PAPER

Stress-induced changes in CARF expression determine cell fate to death, survival, or malignant transformation

Rajkumar S. Kalra[1] · Anupama Chaudhary[1] · Amr Omar[1] · Caroline T. Cheung[1] · Sukant Garg[1] · Sunil C. Kaul[1] · Renu Wadhwa[1]

Received: 9 October 2019 / Revised: 1 March 2020 / Accepted: 6 March 2020 / Published online: 27 March 2020

Abstract

CARF (*C*ollaborator of *ARF*) was discovered as an ARF-interacting protein that activated ARF-p53-p21^{WAF1} signaling involved in cellular response to a variety of stresses, including oxidative, genotoxic, oncogenic, or telomere deprotection stresses, leading to senescence, growth arrest, or apoptosis. Of note, whereas suppression of CARF was lethal, its enrichment was associated with increased proliferation and malignant transformation of cells. These reports have predicted that CARF could serve as a multi-stress marker with a predictive value for cell fates. Here, we recruited various in vitro stress models and examined their effect on CARF expression using human normal fibroblasts. We demonstrate that CARF levels in stress and post-stress conditions could predict the fate of cells towards either death or enhanced proliferation and malignant transformation. We provide extensive molecular evidence that (i) CARF expression changes in response to stress, (ii) it modulates cell death or survival signaling and determines the fate of cells, and (iii) it may serve as a predictive measure of cellular response to stress and an important marker for biosafety.

Keywords CARF · Stress · Survival · Proliferation · Cell transformation · Cell fate

Abbreviations

CARF	Collaborator of ARF
DDR	DNA damage response
UPR	Unfolded protein response
ROS	Reactive oxygen species
CTA	Cell transformation assay
IC	Inhibitory concentration
ER	Endoplasmic reticulum

Electronic supplementary material The online version of this article (https://doi.org/10.1007/s12192-020-01088-y) contains supplementary material, which is available to authorized users.

✉ Sunil C. Kaul
s-kaul@aist.go.jp

✉ Renu Wadhwa
renu-wadhwa@aist.go.jp

[1] AIST-INDIA DAILAB, National Institute of Advanced Industrial Science & Technology (AIST), Tsukuba, Ibaraki 305-8565, Japan

Introduction

CARF (*C*ollaborator of *A*lternative *R*eading *F*rame)/CDKN2AIP is a serine-rich protein, originally identified to be a novel interactor of ARF in the nucleus by yeast two-hybrid screening (Hasan et al. 2002). With its ubiquitous nuclear presence, CARF was found to colocalize with ARF at the periphery of nucleoli and cooperate with the p53 tumor suppressor protein (Hasan et al. 2002, 2004). We had earlier shown that it activates p53 in ARF-dependent and ARF-independent manners (Hasan et al. 2007, 2008). Such activities of CARF-induced activation of p21^{WAF1} function lead to growth arrest and premature senescence in cancer and normal human cells, respectively (Hasan et al. 2009; Cheung et al. 2009, 2010). Suppression of CARF, on the other hand, was lethal and was marked by genomic instability, inhibition of ATR-Chk1 signaling, and cell death (Cheung et al. 2011), implying that it is an essential cell survival protein (Cheung et al. 2011).

Recent studies have shown other functions of CARF, notably in stress response. In cell culture models, a variety of stresses including oxidative, genomic, oncogenic, and telomere erosion

stresses that result in premature senescence are characterized by an increase in CARF along with activation of the p53-p21^{WAF1} axis (Singh et al. 2014). Sato et al. (2015) reported the binding of CARF to XRN2, also known as 5′-3′ exoribonuclease 2 that promoted its translocation from the nucleolus to the nucleoplasm, as a consequence of heat stress. This was supported by the report of Miki et al. (2014) demonstrating that XRN2 binds to PAXT-1, a CARF paralog in *Caenorhabditis elegans* implying that CARF has a major function in stress response and is evolutionary conserved across species. Further, Tsalikis et al. (2016) have shown stress responsiveness of CARF in a model of endoplasmic stress (ER), and Boudreault et al. (2016) found that upregulation of CARF and its isoforms are associated with stress induced by viral infection.

Although the above reports demonstrated an association of CARF with a variety of stresses, the molecular mechanism of its action and outcomes such as growth arrest/apoptosis/survival/transformation have not yet been elucidated. We had earlier reported that CARF levels regulate cell proliferation fates in a dose-dependent manner; whereas overexpression of CARF caused growth arrest, its excessive/super-expression caused malignant transformation (Cheung et al. 2014; Kalra et al. 2015). Further, cells lacking wild-type p53 were malignantly transformed by overexpression of CARF implying that CARF requires p53 to induce growth arrest and its function as a tumor suppressor (Kalra et al. 2015). On the other hand, CARF was found enriched in clinical samples from a variety of cancers suggesting its role in carcinogenesis (Kalra et al. 2018). Of note, its level of expression correlated with poor patient survival in metastatic disease and hence predicted to possess prognostic value (Huang et al. 2015). Concordantly, we demonstrated that the enriched levels of CARF in cancer cells induced EMT by the Wnt/β-catenin axis, and inhibition of CARF decreased both tumor progression and metastasis indicating that CARF may play a major role in carcinogenesis and metastasis via its control of cell fate and lineage (Kalra et al. 2018). Yang et al. (2014) reported that CARF plays a "barrier role" in cellular reprogramming, whereby it functions to suppress cell lineage changes suggesting an essential link between CARF levels and cell fate. In light of these reports, we hypothesized that (i) CARF could be a sensitive and pan-marker of cellular stress and (ii) stress-induced changes in CARF expression could predict cell fate towards apoptosis, senescence, or a cancerous state.

In the present report, we recruited diverse stress conditions to test the utility of CARF as a stress response protein and predictive marker. A variety of chemical stresses were found to alter CARF expression level in human normal cells. Markedly, during the stress conditions, stressors that caused decrease in CARF levels were found to be lethal, while stressors that caused increase in CARF expression triggered growth arrest phenotype. Readouts of CARF levels in stress and post-stress states were further found to be predictive of long-term survival and proliferation state of the cell. Of note, stresses that caused a substantial increase in CARF expression yielded pro-proliferation and cellular transformation phenotypes. Molecular analyses demonstrated that CARF is a new ubiquitous stress marker, regulates stress response and proliferative fate of cells, and hence may serve as an accurate measure of stress and biosafety.

Material and methods

Cell culture

TIG-3 (human diploid embryonic lung fibroblasts) and NIH3T3 (mouse embryonic fibroblasts) cells were obtained from the Japanese Collection of Research Bioresources Cell Bank (JCRB, Tokyo, Japan) and cultured in Dulbecco's modified Eagle's medium (DMEM; Wako, Tokyo, Japan)—supplemented with 10% fetal bovine serum (FBS) and 1% antibiotics in a humidified incubator containing 5% CO_2 at 37 °C, as described earlier (Kalra et al. 2015).

Cell viability and proliferation assay

A total of 5000 cells were seeded in a 96-well plate and treated the following day with various stressors at different concentrations (as shown in Table 1) for different time points (24, 48, 72, and 96 h) as indicated. To examine the cell proliferation in the recovery set (in 48- and 96-well plates), cells were washed thrice with 1× PBS to remove traces of residual toxins before replacing with fresh media. Tetrazolium dye [3-(4,5-dimethylthiazol-2-yl)-2,5-diphenyltetrazolium bromide] (MTT, Invitrogen, Life Technologies, Carlsbad, CA) was used to determine viability of control and treated cells.

Cell morphology observations

Cell morphology of control and treated cells was captured by a phase-contrast microscope (Nikon, Tokyo, Japan), as previously described. Microscopic observation was carried out at × 10 magnification to observe the cell phenotypes induced by the diverse stressors.

Crystal violet staining

Cells from control and treated sets in 6-well and 48-well plates were washed twice with 1× phosphate-buffered saline (PBS) and fixed with ice-cold acetone:methanol (1:1). Subsequently, cells in the plates were stained with 0.1% crystal violet solution, washed thrice, and left open for drying before capturing the images.

Table 1 Table listing details of stresses, concentration (range, $IC_{25–35}$), and biochemical activities caused by their key candidate stressors

Stress types/stressor agents	Drug no.	Candidate stress/chemicals	Diluent/stock diluent	Exp. range	$IC_{25–35}$	Stress response/biochemical activities
Heavy metal (soil, water)	S-01	Sodium(meta)arsenite ($NaAsO_2$	DW	0.5–100 μM	1.5 μM	Protein misfolding/aggregation/hsp induction
Smoke (air)/addictive	S-02	Nicotine ($C_{10}H_{14}N_2$)	NS (0.9% NaCl)	0.2–2 mM	200 μM*	Potent parasympathomimetic stimulant
	S-03	Benzo[a]pyrene ($C_{20}H_{12}$)	DMSO	20–200 μM	40 μM	Mutagenic stressor metabolite/
Air (diesel fuel)	S-04	2-Nitro-9-fluorenone($C_{13}H_7NO_3$)	DMSO	0.1–1 μM	0.1 μM	Mutagenic diesel-exhaust photoproduct
Physiological (anger, emotions)	S-05	Epinephrine ($C_9H_{13}NO_3$)	0.5 M HCl	5–100 μM	20 μM	Hormonic neurotransmitter peptide/steroid
Environmental (plastics)	S-06	Vanadium(v) oxide (V_2O_5)	DW (0.48 M NaOH)	0.4–10 μM	1.2 μM	Amphoteric oxide oxidizing agent
	S-07	Titanium(IV) oxide (TiO_2)	NS (0.9% NaCl)	0.5–5 mM	0.8 mM	Inflammatory/lysosomal activity defects
Environmental (plastics)	S-08	Bisphenol A bis(chloroformate) ($ClCO_2C_6H_4)_2C(CH_3)_2$	DMSO	0.02–200 μM	10 μM	Synthetic xenoestrogen/endocrine disruptor
Polycyclic aromatic HCs	S-09	1-Hydroxypyrene ($C_{16}H_{10}O$)	DMSO	10–100 μM	20 μM	Potent excretory metabolite/PAH exposure
Environmental (soil, water)	S-10	Cadmium nitrate tetrahydrate ($Cd(NO_3)_2{\cdot}4H_2O$)	DW	0.5–5 μM	1.2 μM	Inorganic carcinogen/cytotoxicity
Drug/chemical (chemotherapy)	S-11	Doxorubicin ($C_{27}H_{29}NO_{11}$)	DW	0.125–1.25 μM	0.25 μM	DNA intercalation/DNA damage response
Hypoxia, oxygen deficiency	S-12	Cobalt(II) chloride ($CoCl_2$)	DW	100–1000 μM	500 μM	Inorganic hypoxic substance/erythropoiesis
Radiation, UV	S-13	Ultraviolet (UV) (WL-nm)	-	2.5–25 mJ/cm^2	5 mJ/cm^2	Ionizing radiation/DNA damage
Oxidative damage	S-14	Hydrogen peroxide (H_2O_2)	D-MEM	100–1000 μM	200 μM	Oxidizes proteins, membrane lipids, and DNA
Addiction (alcohol)	S-15	Ethanol (C_2H_6O)	D-MEM	1–10%(*v*/v)	2.5%	Dehydration/hepatic damage
Air, environmental	S-16	Formaldehyde (CH_2O)	1× PBS	150 μM–1.5 mM	200 μM	Organic aldehydes/potent carcinogen

The *denotes Nicotine's 200 μM concentration as an exception in the IC25–35 list. As shown in Fig. S1, nicotine did not cause the inhibitory effect on cell viability; thus * Nicotine's 200 μM concentration does not reflect the Inhibitory Concentration (IC) that was taken in the report. Instead, 200 μM nicotine was chosen as a sub-optimal concentration that has been earlier frequently reported to sufficiently incite the diverse stress signaling pathways in vitro

Cell cycle profiling

Control and stressed cells were harvested by trypsinization, washed with 1× PBS, and fixed in 70% chilled ethanol at 4 °C for 15–30 min. Cells were subsequently incubated with 50 μl ribonuclease A (5 mg/ml; Qiagen, Hilden, Germany) followed by washing at 37 °C for 30 min. Cells were then stained with 250 μl Guava Cell Cycle Reagent (50 mg/ml) in the dark for 1 h and acquired using the Guava Cell Cycle Analyzer (Millipore, Billerica, MA). The data was analyzed by the ModFit LT™ software to check the distribution of cells in different phases of the cell cycle.

Immunoblotting

Cultured cells (80–90% confluency) were harvested with trypsin-EDTA (Gibco, Invitrogen). Harvested cell pellets were lysed in adequate volume of RIPA buffer (Sigma-Aldrich, St. Louis, MO), and proteins were extracted and quantified. Ten micrograms of protein was resolved in SDS-polyacrylamide gel and then electroblotted onto activated PVDF membrane (Millipore) using a semidry transfer unit (ATTO, Tokyo, Japan). Immunoblotting was performed with specific antibodies to Cyclin D1, PARP1, Bcl-xl, Bcl-2, Bax, caspase-3, caspase-9, ATF6α, GST, vimentin, and fibronectin (Santa Cruz, CA); phospho-p44, $p21^{WAF1}$, pATM, HP1γ, Ki-67, XBP1, pJNK/SAPK, PERK, ATF4, Calnexin, and N-cadherin (Cell Signaling Technologies, Danvers, MA); Hsp27, Hsp70, Hsp90, Hsp90α, and Bip/GRP78 (StressMarq Biosciences, Victoria, Canada); and β-actin (Abcam, Cambridge, UK). Antibodies for CARF and Mortalin were raised in our laboratory. PVDF membranes were probed for primary and secondary (HRP-tagged; Santa Cruz) antibodies. Chemiluminescence detection was performed using ECL prime substrate (GE Healthcare, Chicago, IL). Densitometric analysis was performed with ImageJ (NIH, Bethesda, MD), and quantitation of each protein in control and stressed cells was normalized with their respective β-actin level.

Reverse-transcriptase PCR (RT-PCR)

Total RNA from control and stressed cells was extracted using the QIAGEN RNeasy kit. Two micrograms of RNA was used to synthesize cDNA using the ThermoScript® Reverse Transcriptase (QIAGEN) following the manufacturer's instructions. cDNA was then subjected to PCR amplification using transcript-specific set of primers (Table S1) and TaKaRa Ex Taq® DNA polymerase (Takara, Tokyo, Japan). The PCR amplification reactions consisted of an initial 10-min denaturation step at 95 °C, followed by 34 cycles at 95 °C for 45 s, 60 °C for 1 min, and 72 °C for 45 s, and a final 10-min annealing step at 72 °C. Amplified products were resolved on a 1.2% agarose gel containing ethidium bromide (0.5 μg/ml) for visualization.

Immunofluorescence

Cells were harvested and seeded (4×10^4/well) on glass coverslips in a 12-well plate for 24 h. Treatments with various drugs, at indicated concentrations, were given for 48 h followed by fixation with pre-chilled absolute methanol at room temperature (RT)

for 10 min. Cells were next permeabilized with PBS-Triton-X-100 (0.1%) for 10 min followed by blocking with 2% bovine serum albumin (BSA) for 10~20 min, and incubation (RT for 1 h or at 4 °C overnight) with primary antibodies to CARF, Cyclin D1, Ki-67, and PARP1. Coverslips were subsequently incubated with Alexa Fluor–conjugated secondary antibodies (Molecular Probes, Eugene, OR) and counterstained with Hoechst 33258 (Roche, Basel, Switzerland). Immunofluorescence images were observed using a Carl Zeiss Axioplan-2 microscope and acquired with a Zeiss AxioCam HRc camera. Fluorescence intensities of the acquired images were analyzed semiquantitatively using the ImageJ software, normalized to the respective controls, and represented as percentage change over control values.

ROS assay

Cells (40×10^3) were seeded on coverslips placed in 12-well plates for 24 h after which they were treated with the indicated stressors (at $IC_{25–35}$) for 48 h. Subsequently, the treated cells were gently washed with warm 1× PBS and incubated with carboxy-H2DCFDA provided in the Image-iTTM LIVE green reactive oxygen species (ROS) detection kit (Molecular Probes). Cells were then washed thrice with warm 1× PBS and quickly imaged using a Carl Zeiss (Axiovert 200 M) microscope.

SA β-galactosidase senescence assay

Senescence-associated (SA) β-galactosidase senescence assay was performed with the Histochemical Staining Kit (Sigma-Aldrich), as described earlier (Kalra et al. 2015). Staining was observed with a Zeiss Axioplan-2 microscope, equipped with a Zeiss AxioCam HRc camera.

CARF enzyme-linked immunosorbent assay

Fifty microliters of extracted lysates (concentration 20 μg/ml) from stressed and post-stressed recovery cells was prepared with coating and diluent buffers (BioLegend, San Diego, CA), and transferred into clear flat-bottom polystyrene Costar™ 96-well plates (Corning, New York, NY) and incubated at RT overnight. Wells were then washed thrice with washing buffer (0.05% PBS-T) and incubated with anti-CARF antibody (100 ng/ml) prepared in diluent buffer. The plate was incubated at RT overnight, followed by 3× washing and subsequent incubation with secondary HRP antibody (100 ng/ml, Thermo Fisher Scientific, USA) at RT for 3 h. The plate was then washed thrice and incubated with 3,3′,5,5′-tetramethylbenzidine (TMB) substrate (BioLegend) for 15 min for color development. Colorimetric readings were taken at 450 nm using the Infinite M200® Pro microplate reader (Tecan, Männedorf, Switzerland). Recombinant CARF protein was used to prepare the standard curve, and CARF protein concentration in the extracted lysates was calculated as percentage change over the control using the slope equation obtained from the standard.

Cell transformation assay

For cell transformation assay (CTA), two well-established models, namely (i) an NIH3T3-based cell transformation assay and (ii) doxorubicin-induced senescence, in normal human cells were used. In the first model, as described earlier (Hayashi et al. 2008), 2000 cells were seeded in 6-well plates in triplicate and after 24 h, treatments with the selected CARF-inducing stressors (Fig. S8b, taken as tumor-initiation reagent) were given for 48 h in DMEM/F12 medium with 10% FBS. After 48 h (3rd day), the cells were fed with fresh DMEM/F12 medium with 10% FBS and kept for another 4 days (7th day). Then, from days 7 to 17, the cells were fed with medium containing 2 μM insulin in DMEM/F12 + 2% FBS, and the medium was changed every 4 days. From days 17 to 31, the medium containing insulin was changed once a week. On day 31, crystal violet staining was performed, as described in an earlier section, to observe the growth and size of the transformed colonies. In the TIG-3-based cell senescence model, 1.5×10^5 cells were seeded for 24 h after which they were treated with 1 μM doxorubicin for 1 h (day − 5). Subsequently, after treatment, cells were fed with fresh DMEM/F12 medium with 5% FBS and maintained for 5 days to induce premature cell senescence. The pre-senescent cells were then treated with the selected stressors on day 1 and maintained in a similar manner as described for the NIH3T3-based CTA. On day 31, images of the transformed colonies were taken and subsequently SA β-galactosidase staining was performed, as described in an earlier section.

Statistical analysis

All the experiments were performed in triplicates. Obtained data values were expressed as mean ± SEM of three individual experimental sets. Statistical analyses were executed using Student's *t* test or the nonparametric Mann-Whitney *U* test, whichever was applicable. Statistical significance was defined as p value < 0.05. The p values were represented as follows: $*p < 0.05$, $**p < 0.01$, $***p < 0.001$.

Results

Correlation between CARF levels and stress phenotypes induced by diverse stressors

In order to explore the stress-sensing ability of CARF, we examined a variety of stress conditions, using 16 different

chemical agents that we are frequently exposed to in daily life and are known to induce cellular stress (Table 1). We analyzed the cytotoxic potency of these agents by the cell viability assay (Fig. S1), and determined the exposure range to find inhibitory concentrations (IC) at 48 h using normal human fibroblasts, TIG-3 cells (Table 1). As shown in Fig. 1a, sub-cytotoxic concentrations ($IC_{25–35}$) of the diverse stressors had varying effects on CARF expression; a significant decrease in CARF levels was demonstrated in cells treated with S-01, S-09, and S-10, while S-02, S-03, S-04, S-05, S-06, S-12, S-13, and S-16 induced an increase in CARF expression levels. Stress-induced changes in CARF levels were also validated at the transcript levels (Fig. 1a). Stressors S-07, S-08, S-11, S-14, and S-15 at $IC_{25–35}$ concentrations caused no significant alteration in CARF levels and cell phenotype (Fig. S2a–b) and were therefore excluded from subsequent analyses. Semiquantitative analysis of CARF expression by fluorescent immunostaining reaffirmed its varying expression levels induced by the above stressors; no change in localization was noted (Fig. 1b). At sub-toxic levels, these reagents caused distinct stressed morphology in TIG-3 cells as reflected by the changes in cell morphology (Fig. 1c). S-01, S-09, and S-10 induced a contracted/elongated cell shape and reduced cell-to-cell attachments, while cells treated with S-02, S-03, S-04, S-05, S-06, S-12, S-13, and S-16 acquired a flattened and clustered phenotype (Fig. 1c). Of note, stressors, mainly the heavy metals such as sodium (meta)arsenite (S-01) and cadmium nitrate (S-10) and air pollutant such as 1-hydroxypyrene (S-09), i.e., a polycyclic aromatic hydrocarbon (PAH), produced a potent stress phenotype as observed by the presence of shrunken and detached (rounded/translucent) cells (Fig. 1c). Interestingly, all these stressors induced a significant decrease in CARF levels (Fig. 1a, b). On the other hand, stressors such as S-02, S-04, S-05, S-06, S-12, S-13, and S-16 that induced an expanded and flattened morphology resulted in an increase in CARF expression levels (Fig. 1c). Thus,

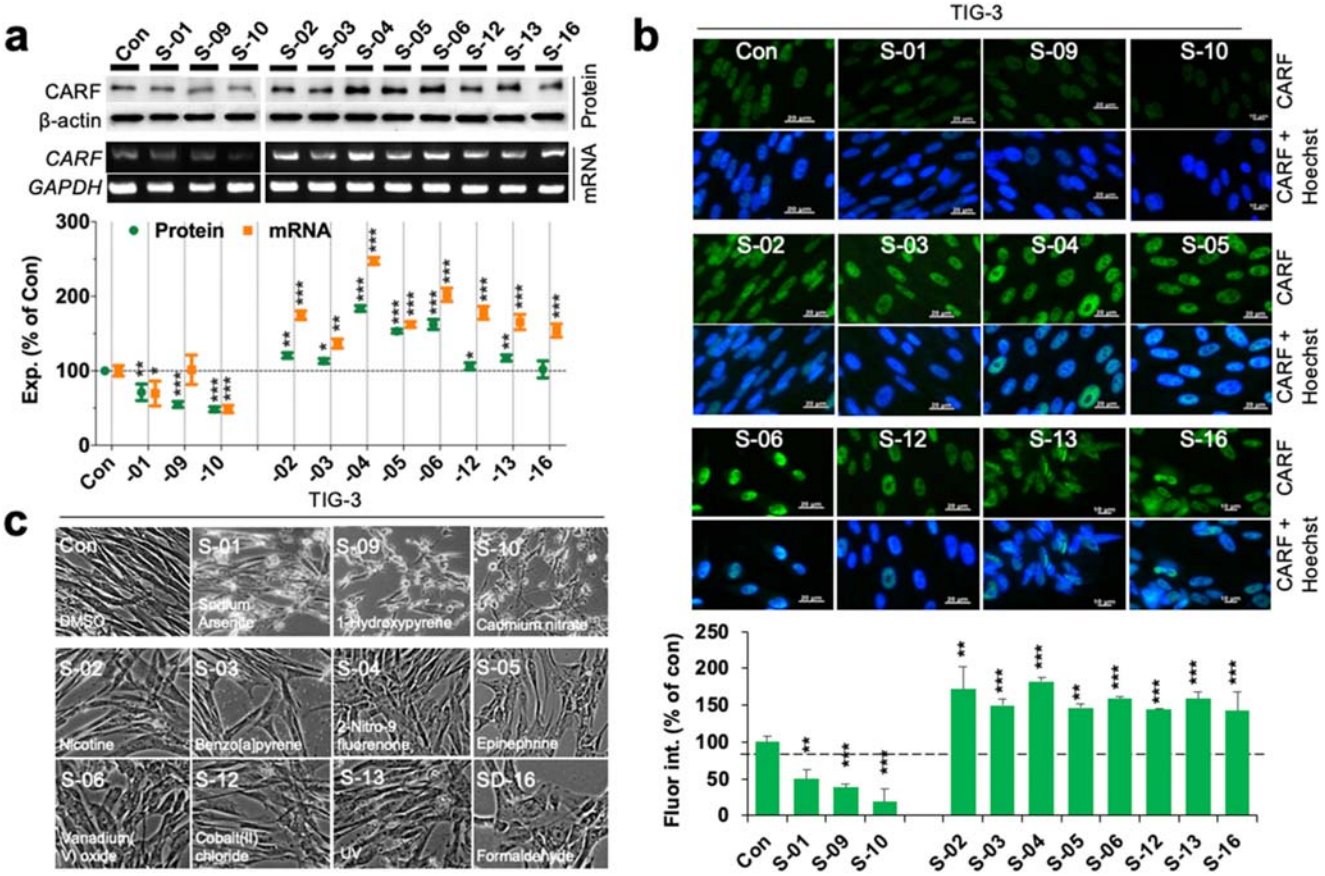

Fig. 1 Correlation between CARF levels and cell stress. **a** Protein and mRNA expression of CARF following treatment with the selected stressors; its level was decreased (S-01, S-09, and S-10) and increased (S-02, S-03, S-04, S-05, S-06, S-12, S-13, and S-16). Quantitation of its protein (green) and mRNA (orange) levels is shown below. **b** Immunostaining showing CARF expression in the normal cells treated with the selected stressors; nuclei are stained blue with Hoechst counterstain; its semiquantitative levels are shown below. **c** Phase-contrast images showing stress phenotype and morphology of cells treated with the selected stressors. Stressors (S-01, S-09, and S-10) were found to cause a shrunken and apoptotic phenotype (marked by round translucent cells), while stressors (S-01–06, S-12, S-13, and S-16) produced a flat and impeded cell phenotype. $*p < 0.05$, $**p < 0.01$, $***p < 0.001$

there was an apparent association between stress phenotype and CARF expression; cells with a flattened cell shape had higher CARF levels, whereas cells with a shrunken shape were marked by reduced CARF levels.

Stress-induced alterations in CARF levels reflect cell survival and proliferative fate

To evaluate the effect of these stressors on cell growth, we first examined the cell cycle profiles of the cells following the stress treatments with sub-cytotoxic concentrations ($IC_{25–35}$) for 48 h (Table 1). As shown in Fig. 2a, stress-induced decline in CARF levels (S-01, S-09, and S-10) was found to be associated with reduced cell survival, as demonstrated by increased apoptosis in these treated cells (Fig. 2a). On the other hand, cells treated with stressors S-02, S-03, S-04, S-05, S-06, S-12, S-13, and S-16 showed growth arrest at the G0/G1 and G2 phases of the cell cycle that suggested a positive correlation between stressed-induced increase in CARF levels and induction of growth arrest. To verify these alterations at the molecular level, we analyzed the expression of markers associated with cell cycle progression, cell survival, and proliferation (Fig. 2b, c). As shown in Fig. 2b, most, but not all, of the stressors that induced upregulation of CARF (S-03, S-04, S-05, S-06, S-12, and S-16) also caused an increase in $p21^{WAF1}$ and growth arrest, consistent with previous results that demonstrated CARF-mediated activation of p53/$p21^{WAF1}$ axis leading to growth arrest (Hasan et al. 2009) (Figs. 1b and 2b). $p21^{WAF1}$ levels in S-01, in contrast to S-09 and S-10, caused an increase in $p21^{WAF1}$ though apoptosis was seen in all of these three stress-induced cells. On the other hand, S-13 did not cause an increase in $p21^{WAF1}$ level, in spite of an evident growth arrest in these cells. Nevertheless, stressors that caused a decrease in CARF (S-01, S-09, and S-10) consistently yielded a decrease in Cyclin D1 (Fig. 2b, c), a major regulator of cell cycle progression. Of note, in S-13-treated cells, increase in CARF was accompanied by an increase in pATM suggesting an activation of UV-induced DNA damage response (DDR) and G0/G1 cell cycle arrest (Fig. 2d). This was further endorsed by an increase in heterochromatin protein 1 (HP1γ), clearly observed in S-02-, S-04-, S-05-, S-06-, S-13-, and S-16-treated cells (Fig. 2d).

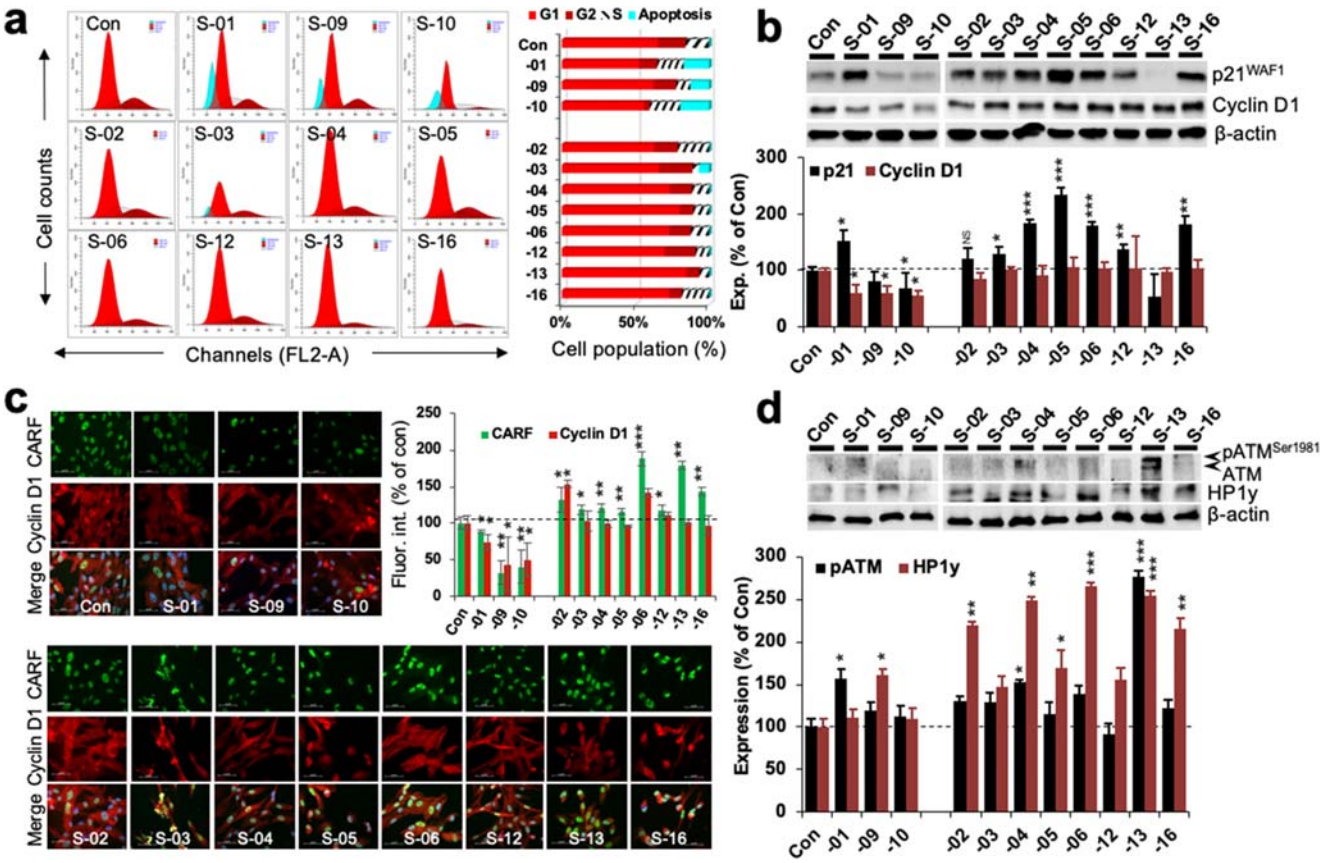

Fig. 2 Stress-induced modulation in CARF levels reflects cell proliferation fates. **a** Cell cycle profiles of cells treated with S-01, S-09, and S-10, and S-02, S-03, S-04, S-05, S-06, S-12, S-13, and S-16 stressors showing apoptosis and growth arrest, respectively. Quantitation of cells in different cell cycle phases is shown on the right. **b** Immunoblots showing $p21^{WAF1}$ and Cyclin D1 expression levels in cells treated with the different stressors. Quantitation is shown below. **c** Immunostaining showing CARF and Cyclin D1 expression in the control and treated cells; their semiquantitative levels are shown below. **d** Immunoblots showing $pATM^{Ser1981}$ and HP1γ expression levels in cells treated with the above stressors. Quantitation is shown below. $*p < 0.05$, $**p < 0.01$, $***p < 0.001$

As shown in Fig. 2a, stressors that caused a decrease in CARF (S-01, S-09, and S-10) promoted apoptosis. Consistent with these results, immunofluorescence staining revealed an increase in the expression of nuclear PARP1, a key apoptotic marker, only in cells treated with S-01, S-09, and S-10. Other stressors yielding growth arrest did not show an increase in nuclear PARP1 (Fig. 3a). Furthermore, Ki-67 (a proliferative cell marker) showed a remarkable decrease in these cells (Fig. 3a). The data was further supported by upregulated levels of Bax, a pro-apoptotic protein, as well as downregulation in the levels of Bcl-2 and Bcl-xl, pro-survival marker proteins (Fig. 3b). Also, a decrease in pro-caspase-9 and cytochrome C (CYCS) at the protein and transcript levels, respectively, affirmed induction of cell death in cells treated with S-01, S-09, and S-10 (Fig. 3b). These results established that the stress-induced decrease in CARF resulted in cell death by apoptosis, supported by earlier reports using CARF overexpressing and knockdown models (Cheung et al. 2014; Cheung et al. 2011). Taken together, we predicted that the stress-induced changes in CARF expression may hold a predictive value to determine cell fate and hence may be important for biosafety evaluation.

CARF is an ubiquitous stress marker

To further elucidate the function of CARF in stressed cells, we analyzed its correlation with markers from established stress signaling pathways. Stressors used in the present study have been shown to induce oxidative/endoplasmic reticulum (ER) stress and/or protein misfolding. Expression analysis of XBP1, JNK/SAPK, and ATF6α, as well as ATF4 and CHOP, downstream effectors of the 3 major axes of ER stress, i.e., Ire1, ATF6, and PERK, respectively, revealed that almost all stressors induced ER stress, as shown by upregulation of XBP1 and ATF6 in almost all groups, independent of the changes in CARF expression (Fig. S3a–b). Of note, expression of ATF6α was the most upregulated in cells treated with stressors S-01, S-09, and S-10 (Fig. S3a). On the other hand, PERK signaling appeared to be inconsistently perturbed, as PERK and CHOP expressions were variably altered by different stressors (Figs. 4a and S3b). Cells treated with stressors S-01, S-09, and S-10 that induced CARF reduction showed an increase in PERK and a decrease in ATF4. On the other hand, stressors that showed CARF upregulation largely had increased ATF4 (Fig. 4a). These results suggested that CARF and ATF4 may be coregulated, independent of PERK/CHOP. On the other hand, BiP or GRP78, a molecular chaperone and downstream target of ATF4, XBP1, and ATF6 transducers, exhibited an increase in response to most of the stressors and was not related to the changes in CARF (Fig. S3a). These data suggested that the stress-induced changes in CARF expression are not directly related to ER stress pathway.

ER stress is tightly linked to protein folding anomalies; thus, we analyzed the proteins involved in the unfolded protein response (UPR) pathway. HSF1, a major regulator of UPR response that acts as a transcription factor and transactivates genes involved in chaperone activity, was found to be transcriptionally upregulated with most of the investigated stressors (Fig. S3b). Furthermore, we found that the heat shock proteins, Mortalin (Mot/GRP75), Calnexin, Hsp90, and

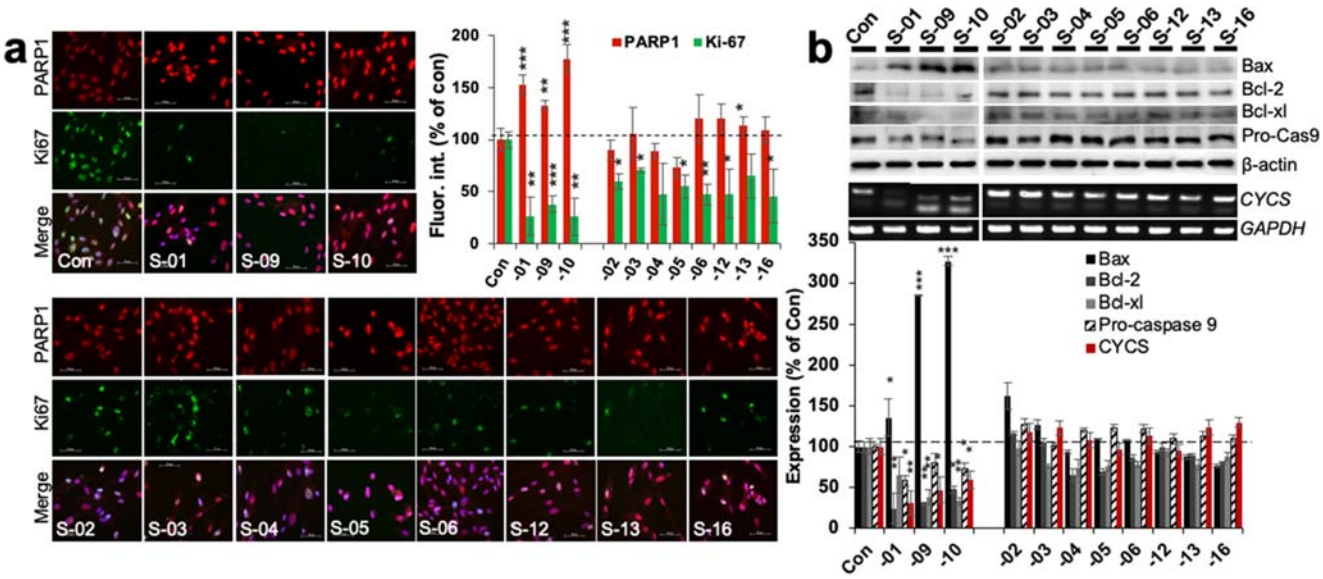

Fig. 3 Stress-induced decrease in CARF levels leads to cell death. **a** Immunostaining showing PARP1 and Ki-67 expression in the normal cells treated with S-01, S-09, and S-10 and S-02, S-03, S-04, S-05, S-06, S-12, S-13, and S-16 stressors; their semiquantitative levels are shown below. **b** Immunoblots and RT-PCR showing Bax, Bcl-2, Bcl-xl, and pro-Cas-9 protein and CYCS mRNA levels in cells treated with the above stressors. Quantitation is shown below. $*p < 0.05$, $**p < 0.01$, $***p < 0.001$

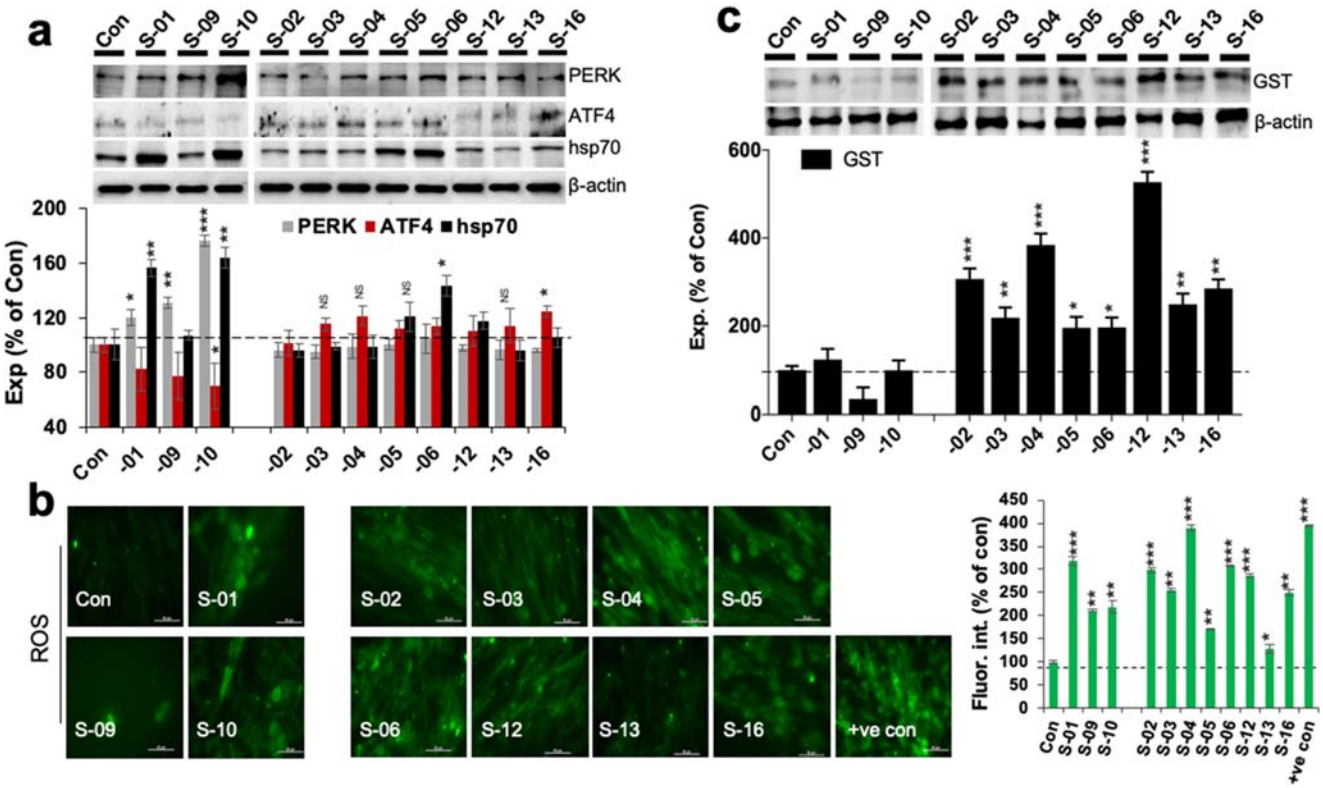

Fig. 4 CARF is an ubiquitous cell stress marker. **a** Immunoblots showing PERK, ATF4, and Hsp70 protein levels in cells treated with S-01, S-09, and S-10 and S-02, S-03, S-04, S-05, S-06, S-12, S-13, and S-16 stressors. Quantitation is shown below. **b** Images showing live fluorescence ROS levels in the treated cells; their semiquantitative fluorescent intensities are shown on the right. **c** Immunoblot showing GST protein levels in control and treated cells. Quantitation is shown below. $^{*}p < 0.05$, $^{**}p < 0.01$, $^{***}p < 0.001$

Hsp27 were ubiquitously activated by all the stressors (Fig. S3c) independently of CARF expression. Interestingly, Hsp70 levels appeared to be inversely associated with CARF levels in some cases; cells treated with stressors S-01 and S-10 showed downregulation of CARF and increase in Hsp70, while the majority of other stressors largely lacked a distinct change in hsp70 levels (Fig. 4a). To examine whether the decrease in hsp70 level was a result of its transcription inhibition, we examined its transcript level (Fig. S3d) and found no significant change in treated Vs control groups. Taken together, these data suggested that the stress-induced changes in CARF expression may not be directly related to ER stress and protein misfolding.

We next examined the association of CARF with markers of oxidative stress. As shown in Fig. 4b, vital staining of cultured control and treated cells showed elevated reactive oxygen species (ROS) levels in most treated cells that was corroborated by an increase in NRF2 and NFκB expression and a decrease in KEAP1 levels (Fig. S4), indicating activation of anti-oxidant response. On the other hand, changes in glutathione S-transferase (GST) protein levels appeared to be closely associated with CARF expression (Fig. 4c). All the stressors that induced CARF upregulation demonstrated a significant increase in GST level too, while cells treated with stressors that caused a decrease in CARF showed either unchanged or lower levels of GST (Fig. 4c). Taken together, it was suggestive that the stress-induced changes in CARF levels did not completely follow the patterns observed for typical ER, UPR, and oxidative stress proteins. However, a close relationship was observed for CARF with ATF4, HSP70, and GST stress marker proteins.

CARF is a predictive measure of post-stress recovery and cell fate in vitro

In order to further investigate the role of CARF in stress response, we examined the association of CARF expression with cell fate in post-stress and recovery states. Cells were treated with sub-lethal concentrations of all 16 different stressors for 48 h and then allowed to recover for 48 h in normal cell culture medium (post-stress recovery period). As shown in Fig. 5a, crystal violet staining of the cells at 48 h of stress treatment and 48 h recovery revealed that cells treated with S-01, S-07, S-09, and S-11 did not recover (Fig. 5a). On the other hand, cells treated with other stressors recovered and sustained growth in the post-stress recovery period. Inspection of cell morphology affirmed stress phenotype in cells treated with stressors S-01, S-07, S-09, and S-11, as marked by

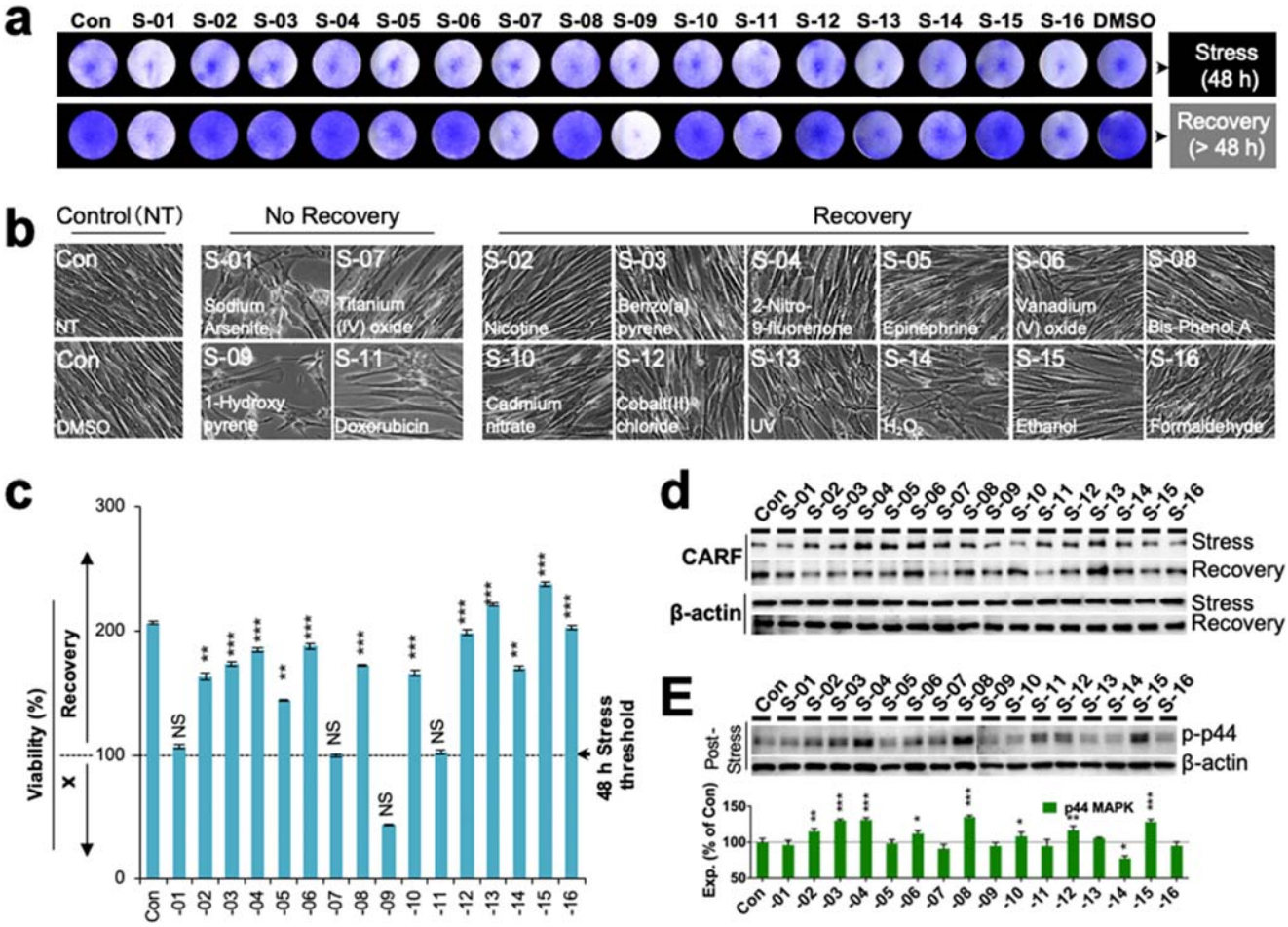

Fig. 5 CARF is a predictive measure of post-stress recovery and cell fate. **a** Crystal violet–stained cells showing proliferation status during stress (48 h) and post-stress (48 h after stress removal, below) recovery following treatment with the 16 stressors. **b** Phase-contrast images showing cell phenotypes 48 h after removal of stress treatments. **c** Cell viability assay showing recovery at 48 h after removal of all stressors, wherein viability of respective sets at 48 h during stress treatment was taken as 100% for analysis. **d** Immunoblots showing CARF protein levels during stress and post-stress recovery. **e** Immunoblots showing p-p44 MAPK protein levels during the post-stress recovery period. Quantitation is shown below

shrunken/irregular shapes, and thereby suggested a lack of recovery (Fig. 5b). These results were corroborated by cell viability readouts (Fig. 5c) at 48-h post-treatment/recovery period as compared with viability at 48 h of stress (considered to be 100%). We next examined the level of CARF by immunoblotting in cells at 48 h of stress and 48 h post-stress, and found that cells treated with stressors S-01, S-07, S-09, and S-11 that had no recovery in terms of cell viability following treatment removal expressed the lowest CARF level (Fig. 5d). These results suggested that cells that were unable to recover the threshold of CARF (required for survival) during recovery period eventually died endorsing that CARF is essential for cell survival. In other words, CARF expression level during post-stress served as a predictive measure of cell fate. Furthermore, expression levels of $p44^{MAPK}$, a cell survival marker, were found to partly corroborate with post-stress restored viability (Fig. 5e). We further assayed the cell senescence in these cells to analyze whether it is associated with restored CARF levels and/or the lack of viability. Increase in CARF levels primarily under stress has been a signature of growth arrest that can lead to senescence if further extended (Hasan et al. 2009; Cheung et al. 2009, 2010). As shown in Fig. 6a, SA β-galactosidase staining demonstrated a relatively higher number of senescent cells in cultures treated with S-13, S-14, and S-16 stresses. Of note, post-stress CARF levels in these cells were comparable with S-6, S-8, and S-10 (Fig. 5d) suggesting that post-stress restoration of CARF level is essentially predictive of cell recovery. However, CARF level beyond a survival threshold may contribute to senescence.

Stress-induced CARF levels potentiate cell transformation and proliferation in the long term

Excessively high CARF levels in cells have earlier been shown to promote pro-proliferation and malignant transformation (Cheung et al. 2014), validated in clinical tumors and

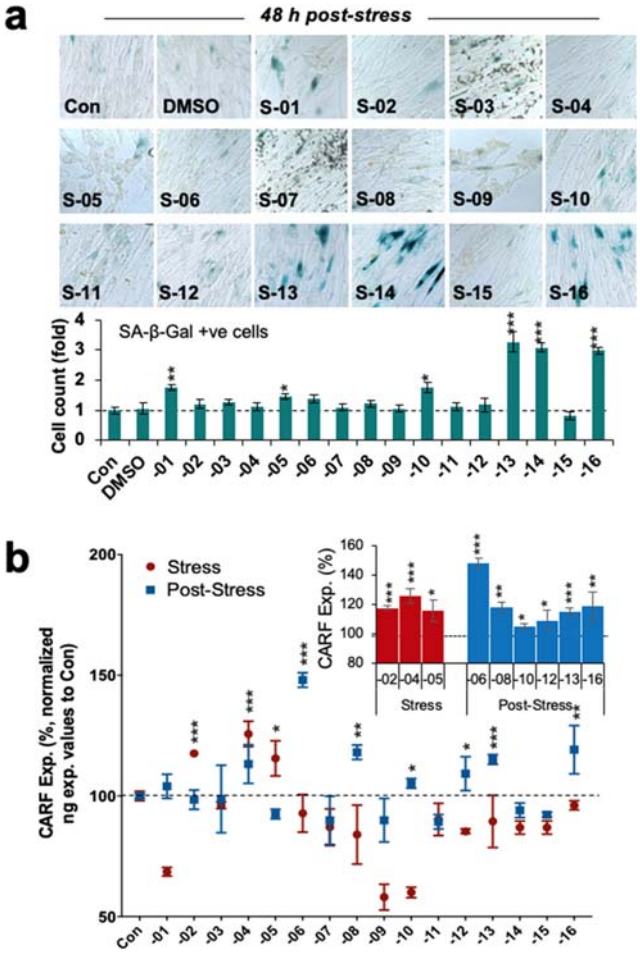

Fig. 6 Restored CARF levels post-stress reflect cell survival and senescence status. **a** Images from senescence-associated β-galactosidase (SA-β-gal) assay showing cell senescence at 48 h after removal of all stressors. Quantitation of β-gal-positive cell counts in fold change is shown below. **b** CARF-based ELISA showing CARF protein levels with all recruited stressors during stress (represented as red) and post-stress (represented as blue) time points. Inset shows selected candidate stressors contributing to CARF levels significantly both during stress (red) and at post-stress (blue) time points

in vitro cell models in multiple reports (Cheung et al. 2014; Kalra et al. 2015, 2018; Huang et al. 2015). In light of these reports, we examined the fate of cells treated with stressors that induced CARF enrichment under stressed and post-stressed conditions. By enrolling a sensitive CARF-based enzyme-linked immunosorbent assay (ELISA) system (Fig. 6b), we found that the stressors S-02, S-04, and S-05 induced immediate and significant enrichment of CARF protein during the stress treatment (represented in red), while S-06, S-08, S-10, S-12, S-13, and S-16 increased CARF during the post-stress recovery period (represented in blue), and therefore were chosen as CARF-inducing stresses (inset plot, showing stress-treated (red) and post-treated/recovered (blue) sets). To investigate the long-term cell growth consequences of such CARF dysregulation induced by stress exposure, we adopted (i) NIH3T3-based cell transformation assay (CTA) and (ii) a cell senescence model of normal human cells (Figs. 7a and S6a), in which the selected stressors that caused enrichment of CARF expression during immediate stress (S-02, S-04, and S-05) and post-stress recovery periods (S-06, S-08, S-10, S-12, S-13, and S-16) (Fig. 6b, inset) were used. As shown in Fig. 7b, exposure to the above stressors produced transformed colonies stained with crystal violet in NIH3T3 cells within 31 days. Cells treated with stressors S-02, S-04, S-06, S-08, S-12, S-13, and S-16 formed large colonies, whereas S-05 and S-10 produced colonies of relatively smaller size. In the untreated control, NIH3T3 cells achieved confluency in the first 7–8 days followed by a decrease in cell number and viability as a result of contact inhibition (Fig. S5a–d), whereas the control group that was given with insulin maintained survival until the endpoint. We then derived sub-lines from the transformed colonies isolated from NIH3T3 CTA for the different stressors, and examined CARF levels by immunoblotting. As shown in Fig. 7c, we observed substantially increased CARF protein in these sub-lines, as compared with the cultured insulin control. However, the sub-line derived from S-10 did not show any difference in CARF expression as compared with the control and other sub-lines, consistent with the reduced size and growth of colonies. Furthermore, we found significantly higher levels of phosphorylated p44 MAPK, a cell proliferative marker that corroborated the observed increase in cell growth of these sub-lines (Fig. 7c). Moreover, these sub-lines were marked with enriched levels of vimentin, N-cadherin, and fibronectin (Fig. 7c), key mesenchymal markers acquired by transformed cells towards attaining malignant invasive and metastatic properties. These results demonstrated that elevated CARF level during or following stress is predictive of transformation ability and metastatic potential in normal cells in the long term.

Consistent with the reports showing that the levels of CARF are upregulated in aged/senescent cells (Hasan et al. 2007, 2009), and as also shown in Fig. 6a, we speculated that exposure to stressors that induced CARF levels may also potentiate transformation in senescent cells. To investigate it further, we used normal TIG-3 cells and modified the CTA scheme by including a 5-day step at the beginning to induce artificial senescence in these cells, as shown in Fig. S6a–c. We found that in these artificially induced senescent cells, exposure to most of the selected stressors acquired cell transformation (Fig. 7d, and data not shown). However, pre-senescent cells treated with stressors S-5 and S-10 showed no cell transformation and therefore suggested a lesser transforming potency of these stresses. To distinguish the transformed colonies from pre-senescent cells, we performed SA β-galactosidase staining. As shown in Fig. 7d, transformed growth could be observed in the pre-senescent cells. Further, analysis of CARF expression in the lysates extracted from transformed TIG-3

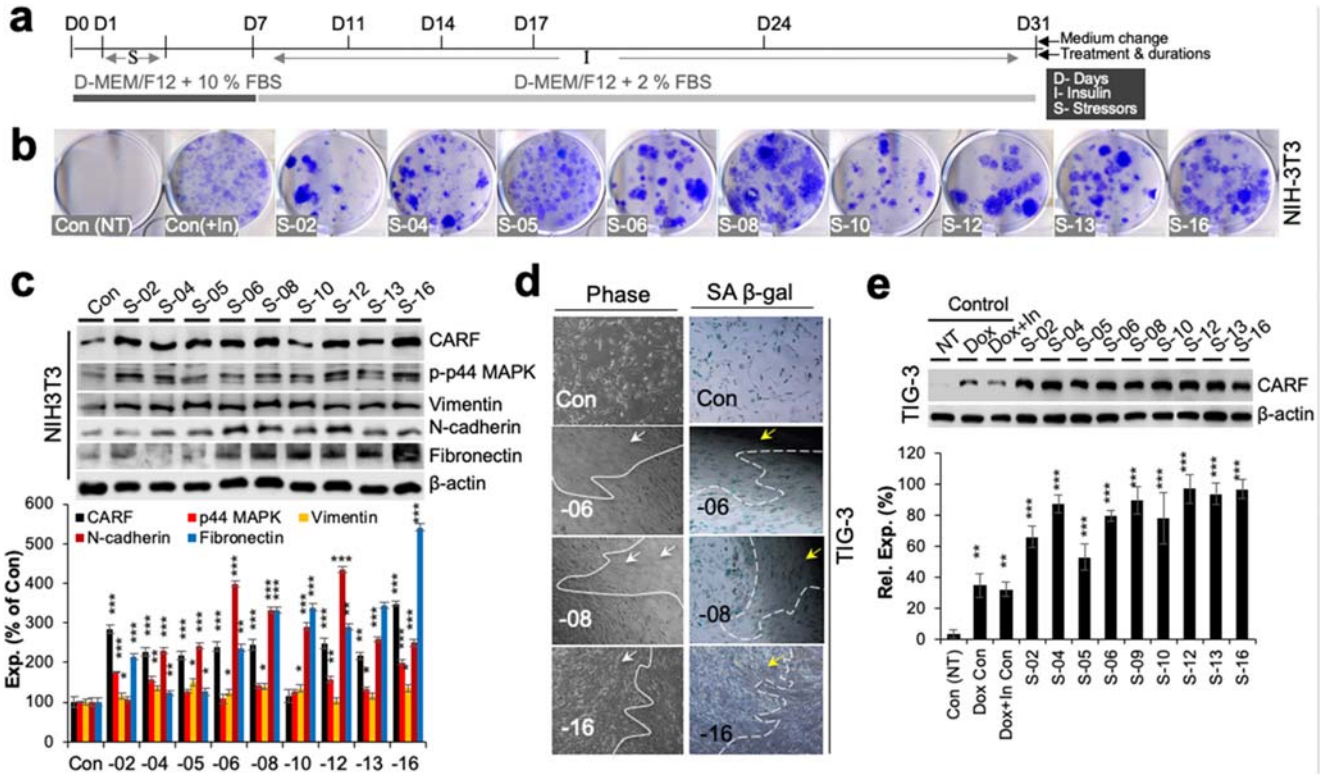

Fig. 7 Stress that upregulates CARF level potentiates cell transformation. **a** Schematic pictorial showing time course of NIH3T3 cell–based cell transformation assay (CTA). D days, I insulin, and S stressors. **b** Images showing crystal violet–stained cells and transformed colonies in con, con(+I), and S-02-, S-04-, S-05-, S-06-, S-08-, S-10-, S-12-, S-13-, and S-16-treated wells, respectively. **c** Immunoblots showing CARF, p-p44MAPK, vimentin, N-cadherin, and fibronectin protein levels in cells derived from NIH3T3 control and transformed clones. Quantitation of their levels is shown below. **d** Phase-contrast and β-gal staining showing cell phenotype and senescence respectively in the representative control, and S-06-, S-08-, and S-16-treated transformed cells; white straight line/dotted line and arrow (white and yellow) mark boundary and position of transformed colonies in phase and β-galactosidase images, respectively. **e** Immunoblot showing CARF protein level in TIG-3 cells derived from control and transformed clones. Quantitation of its level is shown below

colonies reaffirmed the substantial increase in its levels (Fig. 7e). These results confirmed that the exposure to the certain stresses increases CARF levels that can potentiate cell transformation and aggressive proliferation in normal cells in the long term.

Discussion

CARF, by itself or through interaction with ARF, was shown to modulate the p53-HDM2-p21^{WAF1} signaling axis. Activation of the canonical ARF-p53-HDM2-p21^{WAF1} pathway has been a hallmark of genomic stress marked by activation of the DNA damage response (DDR) (Hasan et al. 2002, 2004, 2007, 2008). Upstream induction of CARF in p53-p21^{WAF1} signaling in a replicative stress model previously demonstrated a key role of CARF in cellular stress response leading to growth arrest and senescence (Singh et al. 2014; Hasan et al. 2009). Enhanced CARF levels by oxidative, genotoxic, oncogenic, and telomere deprotection–induced stresses (Singh et al. 2014) have also been pointed to the crucial involvement of CARF in regulating cellular stress responses and its proliferative fate. In contrast, downregulation of CARF protein demonstrated an inevitable lethality (Cheung et al. 2011). On the other hand, substantial enrichment of CARF expression in clinical malignancies has documented its pro-survival and pro-proliferative function in cancer cells (Cheung et al. 2014), validated in in vitro and in vivo models (Kalra et al. 2018). In light of these reports, showing a direct link between CARF levels and cell fate, we speculated that it may play an important role in stress response and serve as a predictive marker for proliferative fate of cells exposed to stress. By enrolling 16 diverse stressors, we found that the stressors causing a decrease in CARF levels caused apoptosis, while those upregulating its levels acquired growth arrest in normal cells (Figs. 1, 2, and 3). Stressors reducing CARF levels such as heavy metals, viz. sodium arsenite (S-01) and cadmium nitrate (S-10), were shown to be the key inducers of ROS, DNA damage, and protein aggregation (Bhagat et al. 2008; Zhang and Reynolds 2019), while 1-hydroxypyrene (S-09) has been shown to cause cytotoxicity by producing DNA lesions (Fullove and Yu 2013). Reduced CARF levels with elevated oxidative and genomic stress conditions caused potent cytotoxicity. These results substantially endorsed the

earlier reports demonstrating that CARF suppression is lethal (Cheung et al. 2014), while its upregulation contributes to growth arrest (Cheung et al. 2009). Of note, S-13-treated cells showed a remarkable decrease in $p21^{WAF1}$ suggestive of its DNA damage–induced degradation to facilitate DNA repair, as reported earlier (Bendjennat et al. 2003; Mansilla et al. 2013). Consistently, distinct activation of ATM (Fig. 2d) was observed that may have mediated growth arrest in these cells. On the other hand, increased $p21^{WAF1}$ levels with sodium arsenite (S-1) suggested arsenite-induced apoptotic function of $p21^{WAF1}$ (Buntharatanapong et al. 2005). These results demonstrated that CARF expression level may serve as a sensitive pan stress response marker with a predictive cell fate value.

We further explored the association of CARF with various stress response pathways including ER, UPR, and oxidative stresses, since the investigated stressors are known to induce these pathways. Analyses of the 3 major axes of ER stress, i.e., Ire1, ATF6α, and PERK (Figs. S3 and S4), revealed that all the investigated stressors induced ER stress, indicating that ER stress response largely functioned independently of CARF levels (Figs. 4, S3). However, an evident coregulated expression of ATF4 with that of CARF was observed (Fig. 4), suggesting possibility of an alternative regulation of ATF4, independent of the PERK/CHOP pathway. This result is particularly interesting because ATF4 is also known as a universal stress response marker that is induced by diverse stresses such as heme deficiency, double-stranded RNA, UPR, hypoxia, and nutrient deprivation through eIF2, independent of the PERK pathway (Shan et al. 2012; Armstrong et al. 2010). Further, recent studies have indicated that ATF4 plays an essential role in regulating cell death/apoptosis (Wortel et al. 2017), Thus, the correlation between CARF and ATF4 may further underline ubiquity of CARF to be a stress response marker with a cell fate predictive value. Besides ER stress, analyses of UPR (BiP, Hsp27, Hsp70, Mortalin, Hsp90, and Calnexin) and oxidative stress (Nrf2, Keap1, GST, Gadd45, NFκb, and NOS2) signaling markers revealed that the investigated stressors also induced these stress response pathways; however, changes in their expression were inconsistent with CARF level, and therefore, these markers lacked a predictive value for cell fate and survival. On the other hand, we observed a close association of Hsp70 and GST with CARF levels. Hsp70 is a highly conserved and ubiquitously expressed heat shock protein that has a vital function in protein folding, cell survival, and protection under stress (Nylandsted et al. 2004; Mosser et al. 1997; Evans et al. 2010). GST is a family of proteins that are known to modulate oxidative stress response and play a key role in extrahepatic drug detoxification (Tew and Townsend 2012; Sau et al. 2010). Therefore, it is suggested that CARF levels may be linked to drug detoxification, and inadequate elimination of the toxins may lead to apoptosis. Taken together, CARF levels along with Hsp70 and GST expression were found to be most closely associated with oxidative stress, suggesting that they could be used as a gene signature for cell fate prediction. In the short-term post-stress period, CARF levels were found to be predictive of post-stress recovery and restored cell viability as well (Fig. 5), and thereby may have a prognostic value as well. Of note, the predictive value of CARF in the post-stress recovery period is independent of the CARF level during stress (Fig. 5d); S-10 had extremely reduced CARF during stress, but in the post-stress recovery period, its expression increased dramatically which was reflected by increased cell viability (Fig. 5a). However, these data largely suggested that post-stress restored CARF levels are essentially predictive of cell recovery/viability (Fig. 5d), and restored CARF levels beyond the survival threshold may trigger cell senescence (Fig. 6a) as shown in earlier studies (Hasan et al. 2009; Cheung et al. 2009, 2010). Interestingly, association of ATF4 and CARF levels in the post-stress period reaffirmed the possibility of an alternative regulation of ATF4 function by CARF.

Gradual increase in CARF expression has earlier been demonstrated for replicative- and stress-induced premature senescence of human fibroblasts (Singh et al. 2014; Cheung et al. 2009, 2010). Meanwhile, excessive enrichment caused malignant transformation of cells that was well marked by activation of Chk2, MAPKs, and mitotic signaling (Cheung et al. 2014; Kalra et al. 2015), which was supported by its enrichment in clinical tumor tissue samples (Kalra et al. 2015). Continuous and long-term stress conditions have been shown to trigger transformation of normal/senescent cells (Kondo et al. 1999; Benhar et al. 2002; Balducci and Ershler 2005; Benz and Yau 2008; Takabe et al. 2001; Krtolica et al. 2001; Adams et al. 2015). Consistent with the reports showing that stress elevated CARF levels (Singh et al. 2014; Tsalikis et al. 2016; Boudreault et al. 2016), we demonstrate that a substantial enrichment of CARF level in stressed cells potentiated their malignant transformation both in mouse and in human fibroblast models (Figs. 6 and 7). These data suggested that stress-induced alterations in CARF level regulate cell fate (induction of senescence/apoptosis/malignant transformation). By cell cycle studies and use of protein synthesis inhibitor (cycloheximide), CARF has been earlier shown to be a short-lived (half-life < 1 h) nuclear protein and is tightly regulated by proteasomal degradation in a cell cycle–dependent manner (Singh et al. 2014). In light of this information, it may be predicted that stress-induced change in proteasomal degradation pathway may contribute to the observed change in CARF expression and warrant further molecular analyses. However, as shown in Fig. 1a, stress-induced change (increase/decrease) in CARF protein was consistent with its mRNA level suggesting that the stress-induced alterations were regulated predominantly at the transcript level. Taken together, in the present study, we report that CARF may serve as a pan-marker for stress and

predictive measure for proliferative states (cell death, senescence, or malignant transformation) of stressed cells.

Author's contributions RSK, RW, and SCK designed the study, interpreted the results, and wrote the manuscript. RSK, AC, AO, and SG performed the experiments and coordinated in result compilation. CTC helped in interpretation of results and manuscript writing.

Funding information The present study is supported by the grants from the Department of Biotechnology (Government of India) and AIST (Japan).

Compliance with ethical standards All experiments were performed according to the approval by institute ethical committee.

Conflict of interest The authors declare that they have no conflict of interest.

References

Adams PD, Jasper H, Rudolph KL (2015) Aging-induced stem cell mutations as drivers for disease and cancer. Cell Stem Cell 16:601–612

Armstrong JL, Flockhart R, Veal GJ, Lovat PE, Redfern CP (2010) Regulation of endoplasmic reticulum stress-induced cell death by ATF4 in neuroectodermal tumor cells. J Biol Chem 285:6091–6100

Balducci L, Ershler WB (2005) Cancer and ageing: a nexus at several levels. Nat Rev Cancer 5:655–662

Bendjennat M, Boulaire J, Jascur T, Brickner H, Barbier V, Sarasin A, Fotedar A, Fotedar R (2003) UV irradiation triggers ubiquitin-dependent degradation of p21(WAF1) to promote DNA repair. Cell 114:599–610

Benhar M, Engelberg D, Levitzki A (2002) ROS, stress-activated kinases and stress signaling in cancer. EMBO Rep 3:420–425

Benz CC, Yau C (2008) Ageing, oxidative stress and cancer: paradigms in parallax. Nat Rev Cancer 8:875–879

Bhagat L, Singh VP, Dawra RK, Saluja AK (2008) Sodium arsenite induces heat shock protein 70 expression and protects against secretagogue-induced trypsinogen and NF-kappaB activation. J Cell Physiol 215:37–46

Boudreault S, Martenon-Brodeur C, Caron M, Garant JM, Tremblay MP, Armero VE, Durand M, Lapointe E, Thibault P, Tremblay-Letourneau M, Perreault JP, Scott MS, Lemay G, Bisaillon M (2016) Global profiling of the cellular alternative RNA splicing landscape during virus-host interactions. PLoS One 11:e0161914

Cheung CT, Singh R, Yoon AR, Hasan MK, Yaguchi T, Kaul SC, Yun CO, Wadhwa R (2011) Molecular characterization of apoptosis induced by CARF silencing in human cancer cells. Cell Death Differ 18:589–601

Cheung CT, Hasan MK, Widodo N, Kaul SC, Wadhwa R (2009) CARF: an emerging regulator of p53 tumor suppressor and senescence pathway. Mech Ageing Dev 130:18–23

Cheung CT, Kaul SC, Wadhwa R (2010) Molecular bridging of aging and cancer: a CARF link. Ann N Y Acad Sci 1197:129–133

Cheung CT, Singh R, Kalra RS, Kaul SC, Wadhwa R (2014) Collaborator of ARF (CARF) regulates proliferative fate of human cells by dose-dependent regulation of DNA damage signaling. J Biol Chem 289: 18258–18269

Evans CG, Chang L, Gestwicki JE (2010) Heat shock protein 70 (hsp70) as an emerging drug target. J Med Chem 53:4585–4602

Fullove TP, Yu H (2013) DNA damage and repair of human skin keratinocytes concurrently exposed to pyrene derivatives and UVA light. Toxicol Res (Camb) 2:193–199

Hasan MK, Yaguchi T, Sugihara T, Kumar PK, Taira K, Reddel RR, Kaul SC, Wadhwa R (2002) CARF is a novel protein that cooperates with mouse p19ARF (human p14ARF) in activating p53. J Biol Chem 277:37765–37770

Hasan MK, Yaguchi T, Minoda Y, Hirano T, Taira K, Wadhwa R, Kaul SC (2004) Alternative reading frame protein (ARF)-independent function of CARF (collaborator of ARF) involves its interactions with p53: evidence for a novel p53-activation pathway and its negative feedback control. Biochem J 380:605–610

Hasan MK, Wadhwa R, Kaul SC (2007) CARF binds to three members (ARF, p53, and HDM2) of the p53 tumor-suppressor pathway. Ann N Y Acad Sci 1100:312–315

Hasan MK, Yaguchi T, Harada JI, Hirano T, Wadhwa R, Kaul SC (2008) CARF (collaborator of ARF) interacts with HDM2: evidence for a novel regulatory feedback regulation of CARF-p53-HDM2-p21WAF1 pathway. Int J Oncol 32:663–671

Hasan K, Cheung C, Kaul Z, Shah N, Sakaushi S, Sugimoto K, Oka S, Kaul SC, Wadhwa R (2009) CARF is a vital dual regulator of cellular senescence and apoptosis. J Biol Chem 284:1664–1672

Hayashi K, Sasaki K, Asada S, Tsuchiya T, Hayashi M, Yoshimura I, Tanaka N, Umeda M (2008) Technical modification of the Balb/c 3T3 cell transformation assay: the use of serum-reduced medium to optimise the practicability of the protocol. Altern Lab Anim 36:653–665

Huang HL, Wu YC, Su LJ, Huang YJ, Charoenkwan P, Chen WL, Lee HC, Chu WC, Ho SY (2015) Discovery of prognostic biomarkers for predicting lung cancer metastasis using microarray and survival data. BMC Bioinformatics 16:54

Kalra RS, Cheung CT, Chaudhary A, Prakash J, Kaul SC, Wadhwa R (2015) CARF (collaborator of ARF) overexpression in p53-deficient cells promotes carcinogenesis. Mol Oncol 9:1877–1889

Kalra RS, Chaudhary A, Yoon AR, Bhargava P, Omar A, Garg S, Yun CO, Kaul SC, Wadhwa R (2018) CARF enrichment promotes epithelial-mesenchymal transition via Wnt/beta-catenin signaling: its clinical relevance and potential as a therapeutic target. Oncogenesis 7:39

Kondo S, Toyokuni S, Iwasa Y, Tanaka T, Onodera H, Hiai H, Imamura M (1999) Persistent oxidative stress in human colorectal carcinoma, but not in adenoma. Free Radic Biol Med 27:401–410

Krtolica A, Parrinello S, Lockett S, Desprez PY, Campisi J (2001) Senescent fibroblasts promote epithelial cell growth and tumorigenesis: a link between cancer and aging. Proc Natl Acad Sci U S A 98: 12072–12077

Mansilla SF, Soria G, Vallerga MB, Habif M, Martinez-Lopez W, Prives C, Gottifredi V (2013) UV-triggered p21 degradation facilitates damaged-DNA replication and preserves genomic stability. Nucleic Acids Res 41:6942–6951

Miki TS, Richter H, Ruegger S, Grosshans H (2014) PAXT-1 promotes XRN2 activity by stabilizing it through a conserved domain. Mol Cell 53:351–360

Mosser DD, Caron AW, Bourget L, Denis-Larose C, Massie B (1997) Role of the human heat shock protein hsp70 in protection against stress-induced apoptosis. Mol Cell Biol 17:5317–5327

Nuntharatanapong N, Chen K, Sinhaseni P, Keaney JF Jr (2005) EGF receptor-dependent JNK activation is involved in arsenite-induced p21Cip1/Waf1 upregulation and endothelial apoptosis. Am J Physiol Heart Circ Physiol 289:H99–H107

Nylandsted J, Gyrd-Hansen M, Danielewicz A, Fehrenbacher N, Lademann U, Hoyer-Hansen M, Weber E, Multhoff G, Rohde M, Jaattela M (2004) Heat shock protein 70 promotes cell survival by inhibiting lysosomal membrane permeabilization. J Exp Med 200: 425–435

Sato S, Ishikawa H, Yoshikawa H, Izumikawa K, Simpson RJ, Takahashi N (2015) Collaborator of alternative reading frame protein (CARF) regulates early processing of pre-ribosomal RNA by retaining

XRN2 (5′-3′ exoribonuclease) in the nucleoplasm. Nucleic Acids Res 43:10397–10410

Sau A, Pellizzari Tregno F, Valentino F, Federici G, Caccuri AM (2010) Glutathione transferases and development of new principles to overcome drug resistance. Arch Biochem Biophys 500:116–122

Shan J, Fu L, Balasubramanian MN, Anthony T, Kilberg MS (2012) ATF4-dependent regulation of the JMJD3 gene during amino acid deprivation can be rescued in Atf4-deficient cells by inhibition of deacetylation. J Biol Chem 287:36393–36403

Singh R, Kalra RS, Hasan K, Kaul Z, Cheung CT, Huschtscha L, Reddel RR, Kaul SC, Wadhwa R (2014) Molecular characterization of collaborator of ARF (CARF) as a DNA damage response and cell cycle checkpoint regulatory protein. Exp Cell Res 322:324–334

Takabe W, Niki E, Uchida K, Yamada S, Satoh K, Noguchi N (2001) Oxidative stress promotes the development of transformation: involvement of a potent mutagenic lipid peroxidation product, acrolein. Carcinogenesis 22:935–941

Tew KD, Townsend DM (2012) Glutathione-s-transferases as determinants of cell survival and death. Antioxid Redox Signal 17:1728–1737

Tsalikis J, Pan Q, Tattoli I, Maisonneuve C, Blencowe BJ, Philpott DJ, Girardin SE (2016) The transcriptional and splicing landscape of intestinal organoids undergoing nutrient starvation or endoplasmic reticulum stress. BMC Genomics 17:680

Wortel IMN, van der Meer LT, Kilberg MS, van Leeuwen FN (2017) Surviving stress: modulation of ATF4-mediated stress responses in normal and malignant cells. Trends Endocrinol Metab 28:794–806

Yang CS, Chang KY, Rana TM (2014) Genome-wide functional analysis reveals factors needed at the transition steps of induced reprogramming. Cell Rep 8:327–337

Zhang H, Reynolds M (2019) Cadmium exposure in living organisms: a short review. Sci Total Environ 678:761–767